STUDY OF THE DYNAMICS OF A ROTATING FLEXIBLE BEAM AND A FLEXIBLE PENDULUM

Fernando S. Buezas[a,c]**, Marta B. Rosales**[b,c]**, Rubens Sampaio**[d] **and Carlos P. Filipich**[e]

[a]*Department of Physics, Universidad Nacional del Sur, Bahï£¡a Blanca, Argentina, fbuezas@gmail.com*

[b]*Department of Engineering, Universidad Nacional del Sur, Bahï£¡a Blanca, Argentina, mrosales@criba.edu.ar*

[c]*CONICET*

[d]*Department of Mechanical Engineering, Pontificia Universidade Catolica do Rio de Janeiro, Rio de Janeiro, Brazil, rsampaio@puc-rio.br*

[e]*Mechanical Systems Analysis Group, FRBB, Universidad Tecnolï£¡gica Nacional, Bahï£¡a Blanca, Argentina,cfilipich@gmail.com*

Keywords: pendulum, rotating flexible beam, gravitational effect, stiffening effect.

Abstract. The dynamic of a flexible beam forced by an imposed rotating around an axis perpendicular to its plane is addressed. Three approaches are dealt with, two related with simplified theories, belonging to the Strength of Materials and the third one using Finite Elasticity. Within the Strength of Materials approaches, the governing equations are derived by superposing the deformations and the rigid motion in the first model, and by stating the stationarity of the *Lagrangian* (including first and second order effects in order to capture the stiffening due to the centrifugal forces) through Hamilton's principle in the second one. Two actions are considered: gravity forces (pendulum) and prescribed rotation. The stiffening effect due to the centrifugal forces is considered only for the beam rotating at high speeds. Comparison of this too models with the equation of Finite Elasticity is carried out. Energy analysis are performed in order to obtain information about the quality of the numerical solution.

1   INTRODUCTION

In the last decade the problem of a plane rotation of a beam has been studied by several authors due to the importance of the problem.

Simo and Vu-Quoc showed that the use of linear beam theory results in a spurious loss of stiffness due to the partial transfer of centrifugal force action to the bending equation. Hence, one should account for geometric stiffening when the imposed rotation is large. To the best of the authors' knowledge, the first study of vibration of rotating beams was published by Schilhansl Schilhans (1958) who analyzed the bending vibration, assuming steady-state revolution and negligible Coriolis force. He derived a formula relating the fundamental bending eigenfrequency with the angular velocity of revolution.

J.M. Mayo (2004) address the issue comparing different formulations. El-Absy and Shabana (1997) study the effect of geometric stiffness forces on the stability of elastic and rigid body modes. A simple rotating beam model is used to demonstrate the effect of axial forces and dynamic coupling between the modes and the rigid body motion. The effect of higher order terms in the inertia forces as the result of including longitudinal displacement caused by bending deformation is examined, in that paper, using several models. In J.Y. Liu (2004) the equations of motion are derived taking into account the foreshortening deformation term, which have geometric stiffening effect on the rigid-flexible coupling dynamics of the system. An influence ratio is employed as a criterion to clarify the application range of the conventional linear modeling method, in which the stiffening effect is neglected in Al-Qaisia and Al-Bedoor (2005), the approach used in that work takes into account the rotating speed and the effect of vibration amplitude. The free bending vibration of rotating tapered beams is investigated by using the dynamic stiffness method in J.R. Banerjee (2006). A clamped-free rotating flexible robotic arm is studied in the paper of Fung and Yau (1999). Hamilton's principle is used to derive the equation of motion of the arm together with the associated boundary conditions and then the power series method is used to solve the differential problem. The paper J.M. Mayo (2004) reviews different formulations to account for the stress stiffening or geometric stiffening effect arising from deflections large enough to cause significant changes in the configuration of the system. In other paper, El-Absy and Shabana (1997)proposes a simple model which demonstrates that there are applications in which the reference motion can have strong dependence on the elastic deformation is used to examine the coupling between the rigid body and elastic modes. All of this papers model the rotating beam with a theory of Strength of Materials (Euler–Bernoulli or Timoshenko equation), taking into account only the transverse strain.

The dynamic of a slender body that is subjected to large displacements can be dealt with the Strength of Materials (SM) Theory (Euler–Bernoulli and Timoshenko equation), or directly with a Theory of Elasticity (Hunter (1983); Truesdell and Noll (1965); Truesdell and Toupin (1960); Fung (1968)). Almost exclusively, the study of rotational dynamics of a beam is studied from the viewpoint of Euler–Bernoulli or Timoshenko equation (SM) for the transverse displacement and deformation. In this work we go beyond this approach. First we add the longitudinal deformation of a rotating-beam model according to the theory SM of Euler–Bernoulli and, second, we propose a model based on the finite elasticity theory of the rotating beam, which allows more complex and realistic phenomena such as dry friction and the nonlinear effects due to large deformations.

In this work, two types of actions applied to the flexible beam are considered. Firstly the beam is only subjected to gravity forces (i.e. the well-known "pendulum", an object that is attached to a pivot point about which it can swing freely) and secondly a rotation of a section

of the flexible beam is imposed at the extreme point (a flexible beam subjected to a prescribed rotation means that the speed of rotation will be imposed at a section, in this case the end from which it hangs).

Both cases will be tackled by the following three approaches: a) SM with a floating frame, b) SM *via* Hamilton's principle including the stiffening contributions and c) Finite Elasticity (in 2D). In the last case, the constitutive equations issue is dealt with in Truesdell and Noll (1965)and Fung (1968), using the Piola-Kirchhoff stress tensor that lead to strongly non-linear equations. The differential equations of motion are developed in Section 2. In Section 3, these equations are presented in weak form and discretized through finite element *via* Galerkin method. The boundary conditions are also discussed since the equations are stated in a *Lagrangian* configuration in the case of Finite Elasticity. The influence of the stiffening effect in the rotating beam motion, in the tree models are compared. Also an analysis of the energy conservation is included (W.M.Lai (1993)) which permits the control of the numerical convergence. We take as a reference NLTE model. In order to compare these results with the literature, we include a section which compares the motion of a 2D pendulum with the paper of Y. Vetyukov and H. Irschik (2004). Section 4 concludes the article.

2   STATEMENT OF THE EQUATIONS OF MOTION

In this section the equations of plane motion of a rotating beam are stated and discussed. Three approaches are presented and compared. The first two are Strength of Materials (SM) model for a one dimension continuum in plane motion and the third one, belong to the 2D non-linear theory of Elasticity (NLTE) that is the beam is a two-dimensions body in planar motion. Whereas the stiffening effect is included naturally in the NLTE approach, in the SM theory a second order effect should be considered to take into account the stiffening effect.

2.1   Linear one-dimensional model (SM)

Two models are stated within the SM theory. One of them is constructed by superimposing a rigid body motion of the beam with small deformation around the rigid configuration J.Y. Liu (2004); Hunter (1983); J.R. Banerjee (2006). The other, stating the stationarity of the *action* (including the second order effects in order to capture the phenomenon of stiffening) through Hamilton's principle. The effect superposition and the Hamilton's principle models will be named Model SM1 and Model SM2.

2.1.1   Model SM1

The governing equations of a beam undergoing plane rotation are stated superposing the equations governing the small deformations of the beam to the ones of the rigid motion J.Y. Liu (2004); Hunter (1983); J.R. Banerjee (2006). That is, let us suppose that the body motion is given by the displacement vector $\mathbf{u} = \mathbf{u}_r + \mathbf{u}_d$ where $\mathbf{u}_r(t) = (u_r(t), v_r(t))^T$ is the rigid part of the motion and $\mathbf{u}_d(X, t) = (u_d(X, t), v_d(X, t))^T$ is the part related with the beam deformation. Then the governing equations are in the floating frame are

$$EA\frac{\partial^2 u_d}{\partial X^2} - \rho A \left(\frac{\partial^2 u_r}{\partial t^2} + \frac{\partial^2 u_d}{\partial t^2} \right) = f_1 \tag{1}$$

$$EI\frac{\partial^4 v_d}{\partial X^4} + \rho A \left(\frac{\partial^2 v_r}{\partial t^2} + \frac{\partial^2 v_d}{\partial t^2} \right) = f_2 \tag{2}$$
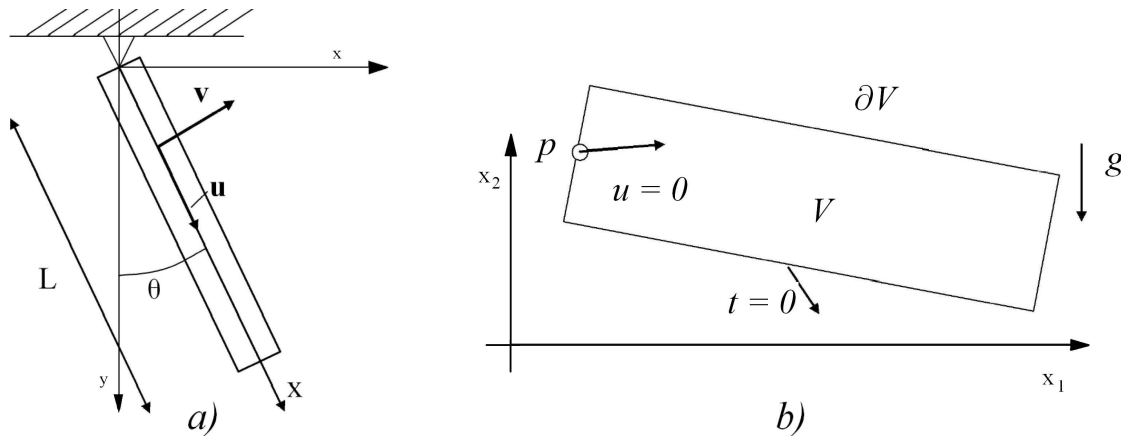
Figure 1: Geometry of the pendulum. a) Displacement vectors (SM); b) Pendulum scheme in the non-deformed configuration (NLTE).

where X is the material coordinate fixed in the frame, t is the time, E is the modulus of elasticity, A is the cross-sectional area of the beam, I is the second area moment, ρ is the volumetric density, $\mathbf{u} = (u, v)^T$ is the displacement vector, u and v are the longitudinal and transverse displacement components, and f_1 and f_2 are the normal and transversely applied forces (gravity components). Now $\mathbf{u}_r$ should be obtained from the equations governing the rigid motion to be replaced in Eq. 2 in order to solve the problem. For instance, in the case of a pendulum of length L and gravity g (see Figure 1), one obtains $\ddot{\theta} + \frac{3}{2L} g \sin\theta = 0$, this equation gives $\theta(t)$, and then, $u_r = X(\sin\theta - 1)$ and $v_r = -X\cos\theta$ can be computed. For example, if $\mathbf{P}$ is a point of rigid at X then

$$\mathbf{P} = X \left(\sin\theta, -\cos\theta\right)^T = X\hat{\mathbf{i}}$$

then

$$\ddot{\mathbf{P}} = X \left(-\dot{\theta}^2\hat{\mathbf{i}} + \ddot{\theta}\hat{\mathbf{j}}\right)$$

were $\hat{\mathbf{i}}$ and $\hat{\mathbf{j}}$ are the versors that generate the mobile frame. Then

$$\frac{\partial^2 u_r}{\partial t^2} = -X\dot{\theta}^2; \qquad \frac{\partial^2 v_r}{\partial t^2} = X\ddot{\theta}$$

2.1.2   Model SM2

This model is derived by stating the *action*. The kinematic transformation equations (Figure 1 *a*) are

$$
\begin{aligned}
x(X,t) &= X\sin\theta + u(X,t)\sin\theta + v(X,t)\cos\theta & (3)\\
y(X,t) &= -X\cos\theta - u(X,t)\cos\theta + v(X,t)\sin\theta & (4)
\end{aligned}
$$

The following four energies contributions are introduced:

$$2W_1 = EA\int_0^L \left(\frac{\partial u}{\partial X}\right)^2 dX + EI\int_0^1 \left(\frac{\partial^2 v}{\partial X^2}\right)^2 dX; \tag{5}$$

$$2W_2 = \int_{(A)}\int_0^1 \sigma\left(\frac{\partial v}{\partial X}\right)^2 dX\, dA \tag{6}$$

$$2K = \rho A\int_0^1 \left(\dot{x}^2 + \dot{y}^2\right) dX \;; \quad P = -\rho g\int_{(A)}\int_0^1 y\, dX\, dA \tag{7}$$

where u, v, x, y are functions of (X,t), W_1 is the strain energy due to axial and bending deformations, K is the kinetic energy, P is the gravitational potential energy and W_2 is the internal work done by the *axial stress* is that arise from the centrifugal effect and the *change of length* due to the bending deformation. The stress due to the centrifugal effect is $\sigma = \rho\omega^2(L^2 - X^2)/2$. This contribution is well-known within the classical Strength of Materials is a second order effect, or $P - \Delta$ effect (yet linear). Bleich and Ramsey (1952) name this contribution as *potential energy of the axial loads*. Consequently the *Lagrangian* is $\mathcal{L} = K - (W_1 + W_2 + P)$ and with this, the Hamilton's principle $\delta \int_{t_1}^{t_2} \mathcal{L} dt = 0$ gives the equations of motion

$$k_L \frac{\partial^2 u}{\partial X^2} - \left(\ddot{u} - \omega^2 u - 2\omega\dot{v} \right) = F(X,t) \qquad (8)$$

$$k_v \frac{\partial^4 v}{\partial X^4} + \left(\ddot{v} - \omega^2 v - 2\omega\dot{u} \right) + \omega^2 \left(\frac{X^2 - L^2}{2} \frac{\partial^2 v}{\partial X^2} + X \frac{\partial v}{\partial X} \right) = G(X,t) \qquad (9)$$

where $\omega = \dot{\theta}$, $k_L = E/\rho$, $k_v = (EI)/(\rho A)$, $F(X,t) = -(\omega^2 X + g\cos\omega t)$, and $G(X,t) = -g\sin(\omega t)$.

2.2   Two dimensional model with finite deformations (NLTE)

2.2.1   Equations of motion

In this Section the equations of the elastic body, in two dimensions for finite displacements and deformations, are stated within the framework of Continuum Mechanics in the *Lagrangian* form, or material representation. Some advantages over the *Eulerian* form, or spatial representation, result in this problem. Now, if the problem is given in the *Lagrangian* form, the only vectorial equation of motion to be solved is

$$\nabla \cdot \mathbf{P} + \rho_0 \mathbf{b} = \rho_0 \mathbf{A} \qquad (10)$$

where $\mathbf{P}$ is the first Piola-Kirchhoff stress tensor and $\nabla \cdot \mathbf{P}$ is the divergence of $\mathbf{P}$ calculated in material coordinates Truesdell and Noll (1965), ρ_0 is the mass density in the reference (already known), $\mathbf{b}$ are the body forces and $\mathbf{A} = \partial\mathbf{V}/\partial t = \partial^2\mathbf{x}/\partial t^2$ where $\mathbf{x} = (x_1, x_2)^T$ is the position vector (spatial coordinate of material point $\mathbf{X}$) and $\mathbf{A}$ is the acceleration field that is simply the partial derivative of the velocity field $\mathbf{V}$). The boundary conditions are imposed over the reference (always known), which together with the initial conditions and the equation of motion, yield a determined problem. All the non-linearities are transferred to the non-symmetric $\mathbf{P}$ tensor. The next relationship relates $\mathbf{P}$ and $\mathbf{\Sigma}$ (the Cauchy stress tensor—spatial description)

$$\mathbf{P} = det(\mathbf{F}) \, \mathbf{\Sigma} \mathbf{F}^{-\mathbf{T}}$$

were $\mathbf{F}$ is the deformation gradient $F_{ij} = \partial x_i / \partial X_j$

2.2.2   Constitutive equation

The following constitutive law between the second Piola-Kirchhoff stress tensor $\mathbf{S}$ (symmetric) ($\mathbf{P} = \mathbf{FS}$)) and finite strain tensor

$$\mathbf{E} = \frac{1}{2} \left(\mathbf{F^T F} - \mathbf{I} \right)$$

is proposed Fung (1968)

$$\mathbf{S}(\mathbf{E}) = \lambda \, tr(\mathbf{E})\mathbf{I} + 2\mu\mathbf{E} \tag{11}$$

in which λ and μ are Lame's-type constants, $\lambda = \nu E^*/(1+\nu)(1-2\nu)$, $\mu = E^*/2(1+\nu)$ and E^* and ν are constants. Eq. (11) is also known as St. Venant-Kirchhoff material model Truesdell and Noll (1965). Additional alternatives of possible constitutive equations are discussed in Filipich and RosalesFilipich and Rosales (2000).

As we can see, $\mathbf{E}$ is a function of the derivatives of $\mathbf{x}$, Then by Eq.(11) $\mathbf{S}$ is also function of the derivatives of $\mathbf{x}$. And the same for the tensor $\mathbf{P}$, Then Eq.(10) is

$$\nabla \cdot \mathbf{P}\left(\mathbf{x}(\mathbf{X}, t)\right) + \rho_0 \mathbf{b} = \rho_0 \frac{\partial^2 \mathbf{x}(\mathbf{X},t)}{\partial t^2}$$

and the goal of this problem is to find the position vector $\mathbf{x}$ (or displacement vector $\mathbf{u} = \mathbf{x} - \mathbf{X}$) for all $\mathbf{X}$ and t subject to the boundary conditions discussed in the next section.

3 NUMERICAL IMPLEMENTATION

The following subsections describe the numerical scheme implemented to solve the equations of motion.

3.1 Variational formulation and Galerkin approximation of model SM1

Let $\phi_j = \left(\phi_j^1, \phi_j^2\right)^T$ be a finite element basis (admissible functions) *i.e. Adm* is a set of trial functions defined as

$$Adm = \left\{ \phi_j \mid \phi_j(0) = 0 \text{ and } \int_0^L \left(\frac{\partial \phi_j^1}{\partial X}\right)^2 dX < \infty, \int_0^L \left(\frac{\partial^2 \phi_j^2}{\partial X^2}\right)^2 dX < \infty \right\}$$

Multiplying Eq.(1) by ϕ_j^1 and integrating by parts, we obtain

$$EA\frac{\partial u_d}{\partial X}\phi_j^1\big]_0^L - \int_0^L \left[EA\frac{\partial u_d}{\partial X}\frac{\partial \phi_j^1}{\partial X} + \rho A p_1 \phi_j^1 \right] dX = 0 \tag{12}$$

were $p_1 = \frac{\partial^2 u_r}{\partial t^2} + \frac{\partial^2 u_d}{\partial t^2} - \frac{f_1}{\rho A}$. In the same way for Eq.(2)

$$EI\left[\frac{\partial^3 v_d}{\partial X^3}\phi_j^2\big]_0^L - \frac{\partial^2 v_d}{\partial X^2}\frac{\partial \phi_j^2}{\partial X}\big]_0^L \right] + \int_0^L \left[EI\frac{\partial^2 v_d}{\partial X^2}\frac{\partial^2 \phi_j^2}{\partial X^2} + \rho A p_2 \phi_j^2 \right] dX = 0 \tag{13}$$

were $p_2 = \frac{\partial^2 v_r}{\partial t^2} + \frac{\partial^2 v_d}{\partial t^2} - \frac{f_2}{\rho A}$.

In the case of a rotating beam, in the pivot point, $X = 0$, the function $\phi_j = \partial_X \phi_j = 0$, $\forall j$, and in the free end, $X = L$, the functions $\frac{\partial u_d}{\partial X} = \frac{\partial^3 v_d}{\partial X^3} = \frac{\partial^2 v_d}{\partial X^2} = 0$, then

$$-EA\frac{\partial u_d}{\partial X}\phi_j^1\big]_0^L = 0$$

$$-EI\frac{\partial^3 v_d}{\partial X^3}\phi_j^2\big]_0^L = 0$$

$$EI\frac{\partial^2 v_d}{\partial X^2}\frac{\partial \phi_j^2}{\partial X}\big]_0^L = 0$$

Then, the goal of this problem is to find $\mathbf{u_d} = (u_d, v_d)^T$ such that

$$
\begin{cases}
u_d, v_d \in Adm \\
\forall \phi_j^1 \in Adm, \Rightarrow \int_0^L \left[EA \frac{\partial u_d}{\partial X} \frac{\partial \phi_j^1}{\partial X} + \rho A p_1 \phi_j^1 \right] dX = 0 \\
\forall \phi_j^2 \in Adm, \Rightarrow \int_0^L \left[EI \frac{\partial^2 v_d}{\partial X^2} \frac{\partial^2 \phi_j^2}{\partial X^2} + \rho A p_2 \phi_j^2 \right] dX = 0
\end{cases}
$$

Now, expanding u and v in terms of ϕ_i

$$
u = \sum_{i-1}^N \phi_i^1(X) C_{i1}(t); \qquad v = \sum_{i-1}^N \phi_i^2(X) C_{i2}(t) \tag{14}
$$

and replacing in Eq.(12) and Eq.(13) we find the matrix form

$$
\mathbf{M\ddot{C}_1 + K_1 C_1 = Q_1}
$$

$$
\mathbf{M\ddot{C}_2 + K_2 C_2 = Q_2}
$$

where

$$
M_{ij} = \rho A \int \phi_i^\alpha \phi_j^\alpha dX; \qquad \alpha = 1,2
$$

$$
K_{1ij} = EA \int \frac{\partial \phi_i^1}{\partial X} \frac{\partial \phi_j^1}{\partial X} dX; \qquad K_{2ij} = EI \int \frac{\partial^2 \phi_i^2}{\partial X^2} \frac{\partial^2 \phi_j^2}{\partial X^2} dX
$$

$$
Q_{1j} = -EA \frac{\partial u_d}{\partial X} \phi_j^1]_0^L + \int \left[f_1 - \rho A \frac{\partial^2 u_r}{\partial t^2} \right] \phi_j^1 dX
$$

$$
Q_{2j} = EI \left[-\frac{\partial^3 v_d}{\partial X^3} \phi_j^2]_0^L + \frac{\partial^2 v_d}{\partial X^2} \frac{\partial \phi_j^2}{\partial X}]_0^L \right] + \int \left[f_2 - \rho A \frac{\partial^2 v_r}{\partial t^2} \right] \phi_j^2 dX
$$

3.2 Galerkin approximation of model SM2

As before, let $\phi_j = \left(\phi_j^1, \phi_j^2 \right)^T$ be a finite element basis with the same properties and using Eq.(14). Multiplying Eq.(8) by ϕ_j^1 and Eq.(9) ϕ_j^2 and then integrating by parts, or directly from $\delta \int_{t_1}^{t_2} \mathcal{L} dt = 0$, we obtain the matrix form

$$
\mathbf{M \left(\ddot{C}_1 - \omega^2 C_1 \right) - 2\omega A \dot{C}_2 + K_1 C_1 = Q_1}
$$

$$
\mathbf{M \left(\ddot{C}_2 - \omega^2 C_2 \right) - 2\omega A \dot{C}_1 + \left(K_2 + K^* \right) C_2 = Q_2}
$$

when

$$
M_{ij} = \int \phi_i^\alpha \phi_j^\alpha dX; \qquad \alpha = 1,2
$$

$$
A_{ij} = \int \phi_i^1 \phi_j^2 dX
$$

$$
K_{1ij} = k_L \int \frac{\partial \phi_i^1}{\partial X} \frac{\partial \phi_j^1}{\partial X} dX; \qquad K_{2ij} = -\omega^2 \int \left(L^2 - X^2 \right) \frac{\partial \phi_i^2}{\partial X} \frac{\partial \phi_j^2}{\partial X} dX
$$

$$K_{ij}^* = k_v \int \frac{\partial^2 \phi_i^2}{\partial X^2} \frac{\partial^2 \phi_j^2}{\partial X^2} dX$$

$$Q_{1j} = k_L \frac{\partial u}{\partial X} \phi_j^1 \big]_0^L - \int F \phi_j^1 dX$$

$$Q_{2j} = \left[- \left(k_v \frac{\partial^3 v}{\partial X^3} + \left(L^2 - X^2 \right) \frac{\partial v}{\partial X} \right) \phi_j^2 \big]_0^L + k_v \frac{\partial^2 v}{\partial X^2} \frac{\partial \phi_j^2}{\partial X} \big]_0^L \right] + \int \left[G - \rho A \frac{\partial^2 v_r}{\partial t^2} \right] \phi_j^2 dX$$

One more time, in the case of a rotating beam, in the pivot point $X = 0$ the function $\phi_j = \partial_X \phi_j = 0 \forall j$ and in the free end $(X = L)$ the functions $\frac{\partial u}{\partial X} = k_v \frac{\partial^3 v}{\partial z^3} + (L^2 - X^2) \frac{\partial v}{\partial z} = \frac{\partial^2 v}{\partial X^2} = 0$ then the boundary conditions are

$$\frac{\partial u}{\partial X} \phi_j^1 \big]_0^L = 0$$

$$- \left(k_v \frac{\partial^3 v}{\partial z^3} + \left(L^2 - X^2 \right) \frac{\partial v}{\partial z} \right) \phi_j^2 \big]_0^L = 0$$

$$\frac{\partial^2 v}{\partial z^2} \frac{\partial \phi_j^2}{\partial z} \big]_0^L = 0$$

3.3 Variational formulation of the problem NLTE

It is very simple to get the variational formulation of equations of motion. Let $\mathbf{W}$ be a test vector field (admissible functions) of variables referred to the body in its non deformed configuration (*Lagrangian* description). Once again, multiplying the equations of motion by $\mathbf{W}$ and integrating over V_0 we get:

$$\int \left(\nabla \cdot \mathbf{P} + \rho_0 \mathbf{b} - \rho_0 \mathbf{A} \right) \cdot \mathbf{W} \, dV_0 = 0 \tag{15}$$

$$\int_{\partial V} \left(\mathbf{t}_0 \cdot \mathbf{W} \right) \, dA_0 + \int \left[\rho_0 \left(\mathbf{b} - \mathbf{A} \right) \cdot \mathbf{W} - \mathbf{P} \cdot \nabla \mathbf{W} \right] dV_0 = 0 \tag{16}$$

where (16) is obtained after integrating (15) by parts (using Greens formula), $\mathbf{t}_0$ is the stress vector. Here ∂V is the boundary of volume V. The surface integral is divided in two parts $(\partial V^1, \partial V^2)$. Suppose than the displacement $\mathbf{u}$, and consequently $\mathbf{x}$ is prescribed in a part of the boundary's surface (∂V^1) (essential boundary conditions) and the stress is given in the other part (∂V^2). In order to incorporate the boundary conditions

$$\mathbf{x} = \bar{\mathbf{x}} \text{ on } \partial V^1 \tag{17}$$

$$\mathbf{t}_0 = \bar{\mathbf{t}}_0 \text{ on } \partial V^2 \tag{18}$$

In the case of non homogeneous essential boundary conditions, the solution $\mathbf{x}(\mathbf{X})$ must satisfy the Eq.(17) on ∂V^1 but the test function $\mathbf{W}$ must satisfy the homogeneous essential boundary condition. Then, in the variational problem (16), the admissible test functions $\mathbf{W}$ are defined as

$$\mathbf{W}(\mathbf{X}) \in Adm_1 = \left\{ \mathbf{W} \mid \mathbf{W} = 0 \text{ on } \partial V^1 \text{and } \int \left(\nabla \mathbf{W} \right)^2 dV_0 < \infty \right\}$$

and the solution $\mathbf{x}(\mathbf{X})$

$$\mathbf{x}(\mathbf{X}, t) \in Adm_2 = \left\{ \mathbf{x} \mid \mathbf{x} = \bar{\mathbf{x}} \text{ on } \partial V^1 \text{and } \int \left(\mathbf{P} \right)^2 dV_0 < \infty \right\}$$

and the natural boundary conditions are automatically imposed (16). Then the surface integral in Eq. (16) reduces to

$$\int_{\partial V} (\mathbf{t}_0 \cdot \mathbf{W}) \ dA_0 = \int_{\partial V^2} \overline{\mathbf{t}}_0 \cdot \mathbf{W} \ dA_0$$

were $\overline{\mathbf{t}}_0$ is the value of the tension $\mathbf{t_0}$ in the boundary.

In the case of a pendulum (beam rotating under gravity) the stress are null on the external body surface with exception to the pivot point p. On the other hand the problem with prescribed motion (beam with prescribed rotation with constant velocity), the stress are null on the external body surface with exception to the the clamped boundary. At these points essential conditions are imposed. In the *Lagrangian* description the stress is given by $\mathbf{t_0} = \mathbf{P} \cdot \mathbf{N}$, where $\mathbf{t_0}$ is the stress vector of Piola–Kirchhoff and $\mathbf{N}$ is the normal vector of the surface in the reference configuration(Figure 1b).

Finally, the variational problem consists to find the vector $\mathbf{x}(\mathbf{X}, t)$ implicit in $\mathbf{P}$ such that

$$\begin{cases} \forall \mathbf{W} \in Adm_1, \text{ find } \mathbf{x} \in Adm_2, \text{ that satisfies} \\ \int_{\partial V^2} (\overline{\mathbf{t}}_0 \cdot \mathbf{W}) \ dA_0 = - \int_V [\rho_0 (\mathbf{b} - \ddot{\mathbf{x}}) \cdot \mathbf{W} - \mathbf{P}(\mathbf{x}) \cdot \nabla \mathbf{W}] \, dV_0 \end{cases}$$

and the initial conditions

$$\mathbf{x}(\mathbf{X}, t_0) = \mathbf{x}_0(\mathbf{X}) \quad \dot{\mathbf{x}}(\mathbf{X}, t_0) = \mathbf{V}_0(\mathbf{X}) \tag{19}$$

3.3.1 Galerkin method and discretization in finite elements

By $\phi \in Adm_1$ a base of a subspace of a Hilbert space. In this paper ϕ_i are a shape vector function. Let the function $\mathbf{x}(\mathbf{X}, t_0)$ be expanded in a series of this vectorial functions $\phi_\mathbf{i}(\mathbf{X})$

$$\mathbf{x}(\mathbf{X}, t) \simeq \sum_{i=1}^{N} \phi_i(\mathbf{X}) \, c_i(t) \tag{20}$$

here $c_i(t)$ are functions only of time. The admissible vector functions are

$$\phi_\mathbf{i}(\mathbf{X}) = [\phi_{x_1 i}(\mathbf{X}), \phi_{x_2 i}(\mathbf{X})]^T$$

Replacing the Eq.(20) in (10) and integrating on the whole domain:

$$\int \left[\nabla \cdot \mathbf{P}(\mathbf{x}) + \rho_0 \mathbf{b} - \rho_0 \left(\sum_{i=1}^{N} \phi_i(\mathbf{X}) \, \ddot{c}_i(t) \right) \right] \cdot \phi_j(\mathbf{X}) \, dV_0 = 0 \tag{21}$$

for j from 1 to n. $\mathbf{P}(\mathbf{x})$ means than Piola - Kirchhoff stress tensor is calculated from $\mathbf{x}(\mathbf{X}, t)$ through constitutive relations (11).

At last, integrating by parts in the general sense, that is using the theorems of vectorial calculus (Greens formula) we get

$$\int_{\partial V_j^2} (\mathbf{t}_0(\mathbf{x}) \cdot \phi_j) \ dA_0 + \int_{V_j} \left[\rho_0 \left(\mathbf{b} - \sum_{\mathbf{i=1}}^{\mathbf{N}} \cdot \phi_\mathbf{i} \, \ddot{\mathbf{c}}_\mathbf{i} \right) \cdot \phi_\mathbf{j}(\mathbf{X}) - \mathbf{P}(\mathbf{x}) \cdot \nabla \phi_\mathbf{j} \right] dV_j = 0 \tag{22}$$

where V_j is the volume of the j-th element.

If the problem has non homogeneous essential boundary conditions, the approximation are

$$\mathbf{x}(\mathbf{X}, t) \simeq \sum_{i=1}^{N} \phi_i(\mathbf{X}) \, c_i(t) + \phi_0(\mathbf{X})$$

where ϕ_0 is known and $\phi_0 = \bar{\mathbf{x}}$ on ∂V^1, and that is why $\mathbf{x} \in Adm_2$.

3.4 Simulation and results

In this subsection the following numerical examples will illustrate the three approaches, as listed next:

1. A flexible beam rotating in a plane, under gravity action is studied using Model SM1, i.e. a Strength of Materials approach with superposition of the beam vibrations of the rigid overall motion.

2. A flexible beam subjected to a prescribed rotation is solved using Model SM2, i.e. a Strength of Materials approach using Hamilton's principle. Since the simulations are done for high speed rotations, the consideration of the stiffening is essential. It was introduced by means of a second order term in the governing functional (Eq. 6).

3. A flexible beam subjected to both a prescribed rotation and gravity is addressed with Model NLTE.

Since the rotating bar is flexible, a flexible beam subjected to a prescribed rotation means that the speed of rotation will be imposed at a point (in this case the end of which hangs).

When dealing with the linear SM models, elements with a sectional cubic finite element basis were employed. Instead, a sectional quadratic polynomial basis was employed to discretized the spatial domain in all the NLTE simulations. Temporal integration was performed using the Gear method (second-order implicit Backward Difference Formula).

3.4.1 The Pendulum

The first example deals with a beam with $L = 5$ m, a square cross-sectional area $A = 0.01$ m^2, Young's-type modulus $E = 4 \cdot 10^7$ N m^{-2}, Poisson-type coefficient $\nu = 0.3$ and mass density $\rho = 7850$ kg/m^3 (Figure 1). The beam is released from a horizontal position with null velocity and restricted to plane motion under a gravitational field. Figure 2a shows the beam motion through the eleven instantaneous configurations during the first second of the motion, corresponding to the Model SM1 and Model NLTE with a 2D discretization. Also the energy variation is depicted in Figure 2b. It is seen that the total energy remains constant, a necessary condition for the numerical solution since we are dealing with a conservative system. The total energy E_t is the sum of the kinetic, elastic strain and potential energies, i.e. $E_t = T + U_e + U_g$ with $T = \frac{1}{2} \int \rho_0 \mathbf{V} \cdot \mathbf{V} \, dV_0$, and $U_g = g \int \rho_0 x_2 \, dV_0$. It can be proved that for the constitutive law (11), it takes the form of the elastic energy as

$$U_e = \int \left[\frac{\lambda}{2} tr(\mathbf{E})^2 + \mu \, tr(\mathbf{E} \cdot \mathbf{E}) \right] dV_0$$

The number of finite elements and the time step were adjusted after an error study. For this purpose the error was defined as follows

$$error = \frac{100}{L} \int_V \left[(x_1^m - x_1^{m'})^2 + (x_2^m - x_2^{m'})^2) \right] dV_0 \tag{23}$$
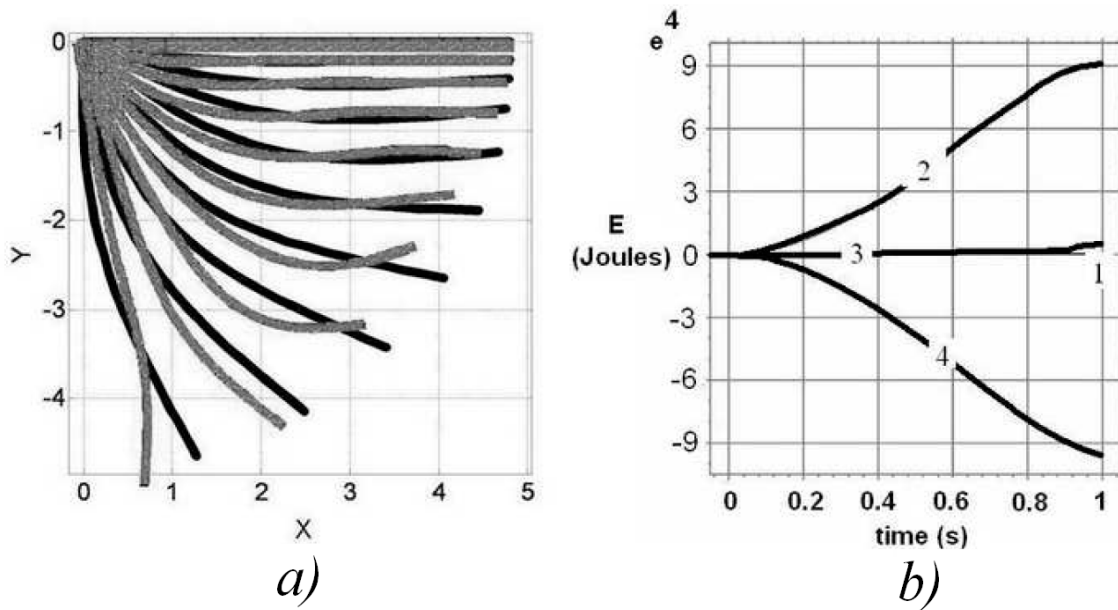
Figure 2: Example 1. Configuration of the bar at different times. Plots at time intervals $\Delta t = 0.1$ s. a) Model SM1 (dark line) and Model NLTE (2D) (clear line). b) Energy in joules (J) as function of time. (1) Total energy, (2) kinetic energy, (3) strain energy and (4) gravitational potential energy.

Simulated time (s)	CPU time (s)		
	1D (SM2)	2D (NLTE)	Ratio 2D/1D
1	10	158	15.8
2	19	304	16

Table 1: Duration of numerical experiments with 1D and 2D simulations. Time in seconds.

Superscript m denote the present numerical experiment and superscript m' a reference solution. The reference case was performed with a hundred times more elements and a time step $1/100$ smaller than the m case. The aim was to yield results with errors less that 1% in $t = 1$ s. The computational, or CPU, time of the reference experiment to simulate 1 s was approximately 12500 s. The duration of other experiments are depicted in Table 1.

3.4.2   Beam subjected to prescribed rotations

The numerical simulation of the dynamics of a beam subjected to prescribed rotations is now presented. The beam length is $L = 1$ m, the cross-sectional area is 0.01 m^2, the prescribed angular velocity is $\omega = 3000$ rad/s, the Young's modulus is $E = 2.1 \cdot 10^{11}$Nm^{-2}, the mass density $\rho_0 = 7850$ kg/m^3 and Poisson's coefficient $\nu = 0.3$. In particular, a large value of ω was assumed in order to obtain large deformations. Thus, the differences between the two approaches could be made apparent. The beam starts its motion from a zero reference (null displacement) and its initial velocity is the one resulting from the angular speed. That is, the beam begins its movement from a horizontal position ($\mathbf{x} = \mathbf{X}$) with a speed given by $V_1 = 0$ and $V_2 = X_1\omega$. The results and comparisons are depicted in Figures 3 and 4. The temporal variation of the coordinate x at the free end of the beam during the motion is plotted in Figure 3 in which the values were found with Model SM1, Model SM2 and Model NLTE (2D). The curves are qualitatively similar though the response found with SM exhibit larger peaks than
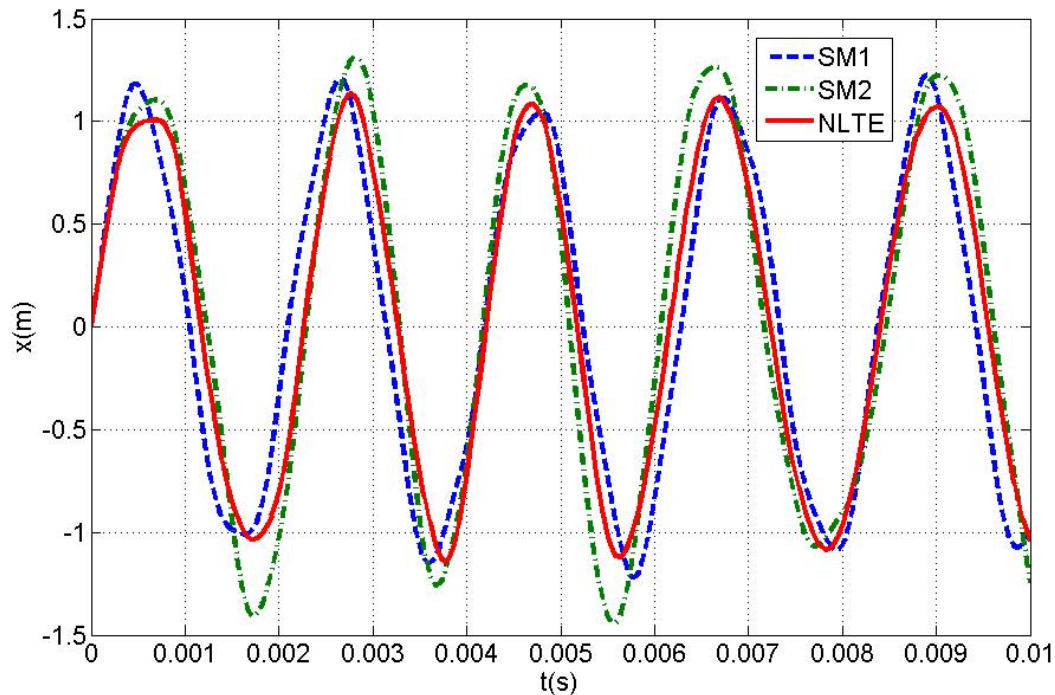
Figure 3: Example 2. Comparison of Models SM1, SM2 and NLTE (2D). Temporal variation of coordinate x at beam tip.

the NLTE model results. It can be observed that the NLTE leads to a stiffer response. Probably this could be explained due to the choice of a linear *Lagrangian* constitutive law —$\mathbf{S}(\mathbf{E})$. If the second Piola-Kichhoff stress tensor $\mathbf{S}$ is transformed into the Cauchy stress tensor Σ, a stiffening behavior with respect to the SM model would arise. This peculiarity is then, not due to the rotation event but to the chosen constitutive model. Figure 4 depicts the variation of the vibration frequency (nondimensionalized with respect to the corresponding frequency at $\omega = 0$) when the rotating velocity is increased. The Model SM1 results are shown in dashed lines, the SM2 are shown in dashed-dot line and the NLTE model in full lines. The results are evidently very close in the cases SM2 and NLTE. The case SM1 is indifferent to the rotation speed as follows directly from Eq. (2). Unlike the case SM2 plotted in Fig. 4 , the velocities were assumed small so as to show that the stiffening is not only consistent with the observed physical behavior but that it is also consistent with NLTE model, in the range of small deformations. For example, the difference in the frequencies between SM2 and NLTE when $\omega = 50$ rad/s are 5% for the first mode, 7% for the second one, 11% for the third one, 14% for the fourth one and 11% for the fifth one. Similar differences are found when $\omega = 0$.

3.4.3 Comparison of NLTE model with data published for the case of a pendulum

Results found with the NLTE model of the present work are contrasted with results reported in Y. Vetyukov and H. Irschik (2004) in which the floating frame of reference approach is used for the analysis of the in-plane oscillations of a suspended rectangular plate. The approach and the computations are different in reference Y. Vetyukov and H. Irschik (2004) and in the present work although the same formal theory is used. In Y. Vetyukov and H. Irschik (2004) the rotation of the frame attached to the body is represented with one rotational degree of freedom.
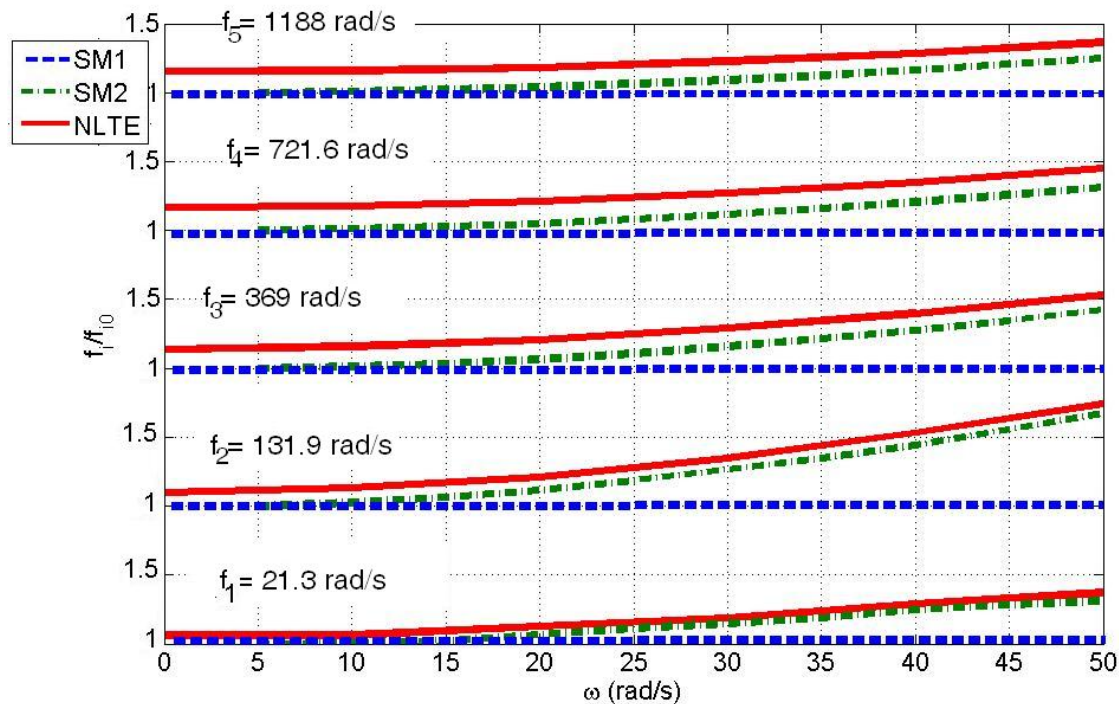
Figure 4: Comparison of Models SM1, SM2 and NLTE (2D). Variation of the first five frequencies with ω.

Besides, a set of continuous polynomial shape functions form the Ritz approximation of the deformation of the body. In the present study, no floating frame is employed and a quadratic finite element basis is chosen for the Galerkin discretization. The plate (or beam) dimensions are $L = 4$ m and a cross sectional area of 1 m^2, mass density ρ_0=7800 kg/m^3, $\nu = 0.3$, $E = 4 \cdot 10^7$ N/m^2. The beam was released from the horizontal undeformed position and then freely oscillated in the gravitational field. An interesting comparison was made regarding with the rotation angle. Given the approach used in Y. Vetyukov and H. Irschik (2004) the angle that rotates the beam is an independent variable and then its value is solved for each time instant. In the present study this angle is not direct result of the calculations. To compare withY. Vetyukov and H. Irschik (2004) the angle was measured at each instant as the slope of the straight line that joins the midpoints of both end cross-sections. Figure 5a shows the angle vs. time reported in Y. Vetyukov and H. Irschik (2004), Fig. 5b plots the resulting angle from the present study and Fig 5c , the superposition of both results. As can be observed, and notwithstanding the diverse methodologies, the excellent agreement yields in Figure 5.

4 FINAL COMMENTS AND CONCLUSIONS

This work has presented a brief review of the open literature on the geometric stiffening of rotating flexible beams. Some of the several methodologies proposed in the literature to account for the stiffening effect in the dynamics equations were analyzed. The dynamics of a flexible beam under gravity (pendulum) and with a prescribed rotation were addressed with models of Strength of Material (SM) and the finite Elasticity (Model NLTE). The SM approach was performed with two models, superposition of motions (Model SM1) and Hamilton's principle (Model SM2). The latter included the stiffening effect. In the case of the superposition model, the equations resulted partially coupled. That is, only the deformation equations are coupled
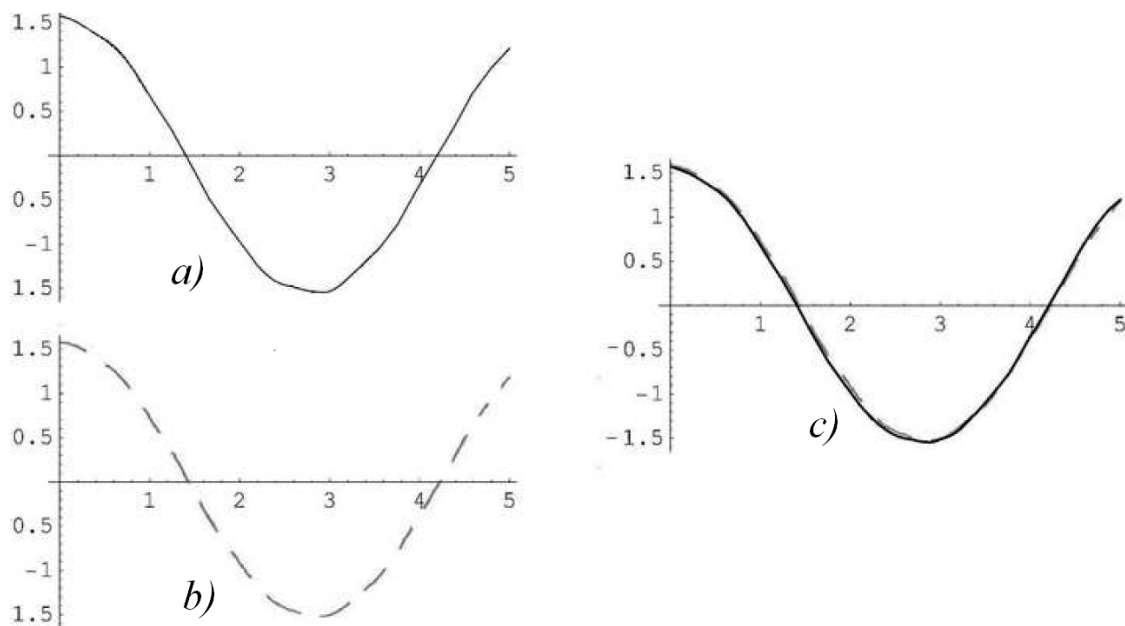
Figure 5: Comparison of Models NLTE (present study) and reference [12]. Temporal variation of rotation angle. a) reference [12]; b) present study; c) superposition of a) and b).

with the rigid motion but the rigid motion equations are uncoupled with the deformations. This derived from the type of construction. The non-linearity is only present in the rigid body motion. On the other hand, when applying Hamilton's principle, fully coupled equations arose. When the beam is subjected only to gravity, model NLTE yielded similar results to the ones obtained with SM theory (Model SM1). However, in the second example, since a very flexible beam with high rotational velocity was studied, the resulting deformations were not small, and consequently the response was not identical. Obviously, as more flexible is the body more differences are found between the linear and nonlinear models.

A flexible beam undergoing low speed prescribed rotation was also studied. The stiffening effect in Model SM2 makes it possible to find almost coincident values of frequencies found *via* finite deformation Model NLTE. As is known the vibration frequencies of a rotating beam increase as the angular velocity ω does which is associated with the stiffening effect introduced by the rotation. In the linear one-dimensional theory (Model SM2) the stiffening effect is due to the contribution of the second order work done by the axial stress caused by the centrifugal force over the bending deformation. For the general case of the dynamics of the elastic body considering finite deformation theory of elasticity, it is not necessary to introduce additional terms in the equation of motion. That is, in the SM2 theory could not only model the effect of stiffening due to centrifugal force, but when compared with the analogue given by NLTE can be concluded that the, stiffening law is the correct. In the conservative pendulum case, the total energy composed of the gravitational, strain and kinetic parts remains constant in time. This is useful to check that the integration scheme introduces neither numerical damping nor instabilities in the solutions. The justification for using the full NLTE model, is that it includes all effects. Obviously the CPU times are larger. Besides it allows to tackle large deformations that can occur with very flexible beams and high rotational speeds. Furthermore other complexities such a finite dimensional pivot can be tackled by this approach. This case also includes the phenomenon of friction in the pivot responsible for the so-called *stick and*

slip. The energy review allows, in this latter case, understanding how energy is dissipated in a flexible pendulum body.

REFERENCES

Al-Qaisia A. and Al-Bedoor B. Evaluation of different methods of the consideration of the effect of rotation on the stiffening. *Journal of Sound and Vibration*, 280:531–553, 2005.

Bleich F. and Ramsey L. *Buckling Strength of Metal Structures*. New York,McGraw-Hill, 1952.

El-Absy H. and Shabana A.A. Geometric stiffness and stability of rigid body modes. *Journal of Sound and Vibration*, 207(4):465–496, 1997.

Filipich C. and Rosales M. A further study on the post-buckling of extensible elastic rods. *International Journal of Nonlinear Mechanics*, 35:997–1022, 2000.

Fung E.H.K. and Yau D.T.W. Effects of centrifugal stiffening on the vibration frequencies of a constrained flexible arm. *Journal of Sound and Vibration*, 224(5):809–841, 1999.

Fung Y. *Foundations of solid mechanics*. Prentice-Hall, 1968.

Hunter S.C. *Mechanics of continuous media*. Ellis Horwood, 1983.

J.M. Mayo D. Garcia-Vallejo J.D. Study of the geometric stiffening effect: Comparison of different formulations. *Multibody System Dynamics*, 11:321–341, 2004.

J.R. Banerjee H. Su D.J. Free vibration of rotating tapered beams using the dynamic stiffness method. *Journal of Sound and Vibration*, 298:1034–1054, 2006.

J.Y. Liu J.H. Geometric stiffening effect on rigid-flexible coupling dynamics of an elastic beam. *Journal of Sound and Vibration*, 278:1147–1162, 2004.

Schilhans M. Bending frequency of a rotating cantilever beam. *Journal of Applied Mechanics*, 25:28–30, 1958.

Truesdell C. and Noll W. *The non-linear field theories of mechanics*. Encyclopaedia of Physics, Vol. III/3,Springer Verlag, 1965.

Truesdell C. and Toupin R. *The Classical Field Theory*. Encyclopaedia of Physics Vol. III/1,Springer Verlag, 1960.

W.M.Lai D. Rubin E.K. *Introduction to continuum mechanics*. Oxford, New York, Butterworth Heinemann, 1993.

Y. Vetyukov J.G. and H. Irschik ". ... The comparative analysis of the fully nonlinear, the linear elastic and consistently linearized equation of motion of the 2d elastic pendulum. *Computers and Structures*, 82:863–870, 2004.